EARTHQUAKE ENGINEERING AND STRUCTURAL DYNAMICS
Earthquake Engng Struct. Dyn. 2003; **32**:265–289 (DOI: 10.1002/eqe.223)

The rocking spectrum and the limitations of practical design methodologies

Nicos Makris*,† and Dimitrios Konstantinidis

Department of Civil and Environmental Engineering, University of California, Berkeley, CA 94720-1710, U.S.A.

SUMMARY

This paper is concerned with the superficial similarities and fundamental differences between the oscillatory response of a single-degree-of-freedom (SDOF) oscillator (regular pendulum) and the rocking response of a slender rigid block (inverted pendulum). The study examines the distinct characteristics of the rocking spectrum and compares the observed trends with those of the response spectrum. It is shown that the rocking spectrum reflects kinematic characteristics of the ground motions that are *not* identifiable by the response spectrum. The paper investigates systematically the fundamental differences in the dynamical structure of the two systems of interest and concludes that rocking structures cannot be replaced by 'equivalent' SDOF oscillators. The study proceeds by examining the validity of a simple, approximate design methodology, initially proposed in the late 1970s and now recommended in design guidelines to compute rotations of slender structures by performing iteration either on the true displacement response spectrum or design spectrum. This paper shows that the simple design approach is inherently flawed and should be abandoned, in particular for smaller, less-slender blocks. The study concludes that the exact rocking spectrum emerges as a distinct intensity measure of ground motions.

KEY WORDS: rocking, uplift, seismic response, earthquake engineering

INTRODUCTION

Reconnaissance reports following strong earthquakes include the uplift, rocking, or overturning, of a variety of slender structures such as tombstones, electrical equipment, retaining walls, liquid storage tanks, and rigid building structures. The need to understand and predict these failures in association with the temptation to estimate levels of ground motions by examining whether slender structures have overturned or survived the earthquakes, has motivated a

* Correspondence to: Nicos Makris, Department of Civil and Environmental Engineering, University of California, Berkeley, CA 94720-1710, U.S.A.
† E-mail: makris@ce.berkeley.edu.

Contract/grant sponsor: National Science Foundation; contract/grant no: CMS-0110354.

Received 22 October 2001
Revised 15 February 2002 and 16 May 2002
Accepted 16 May 2002

number of studies on the rocking response of rigid blocks [1,2,3,4,5,6,7 amongst others and references reported therein].

The first systematic study on the dynamic response of a rigid yet slender block supported on a base undergoing horizontal acceleration was presented by Housner [2], who examined the free- and forced-vibration responses to rectangular and half-sine pulse excitations. Using an energy approach, he presented an approximate analysis of the dynamics of a rigid block subjected to a white-noise excitation, uncovering a scale effect that explained why the larger of two geometrically similar blocks could survive the excitation while the smaller block topples.

The publication of Housner's paper in conjunction with the realistic possibility that building structures may uplift and rock during seismic loading motivated further studies on the seismic response of structures free to rock on their foundations. Priestley *et al.* [8] presented early experimental studies on a model slender structure in an attempt to: (a) validate some of Housner's theoretical results; and (b) to develop a practical methodology to compute displacements of the centre of gravity of the structure due to rocking motion by using standard displacement and acceleration response spectra. Unfortunately, the Priestley *et al.* [8] study is based on the sweeping—and, as will be shown, erroneous—assumption that '*it is possible to represent a rocking block as a single-degree-of-freedom* (*SDOF*) *oscillator with constant damping*, *whose period depends on the amplitude of rocking*'. The unsubstantiated analogies and oversimplified methodologies proposed in the Priestley *et al.* paper are revisited in depth herein since they have been adopted without sufficient scrutiny by the FEMA 356 document: *Prestandard and Commentary for the Seismic Rehabilitation of Buildings* [9].

Figure 1 (top) shows the schematic of the two SDOF structures at their deformed configurations when subjected to ground shaking. The response quantities of interest for the SDOF oscillator are its relative displacement, u, and its time derivatives. The corresponding quantities of interest for the rocking block are its rotation, θ, and its first time derivative—that is the angular velocity, $\dot{\theta}$. In parallel to the response spectra, the paper advances the concept of rocking spectra which are plots of the maximum rotation, θ, and maximum angular velocity, $\dot{\theta}$, versus the frequency parameter (or its inverse) of geometrically similar blocks (with same width-to-height ratio). The paper shows that the rocking spectrum is a distinct and valuable intensity measure of earthquakes and offers information on the earthquake shaking that is not identifiable by the response spectrum of an SDOF oscillator.

ASSUMPTIONS AND JUSTIFICATIONS

When a rigid block is rocking, it is assumed that the rotation continues smoothly from point O to O'. This constraint in conjunction with conservation of angular momentum requires an energy loss during impact that emerges from the requirement that the block sustains rocking motion. The minimum energy loss during impact depends on the slenderness of the block. An energy loss during impact that is greater than the minimum energy loss required for the realization of rocking motion will result in more rapid decay of the vibrations. Conversely, an energy loss during impact that is less than the aforementioned minimum energy

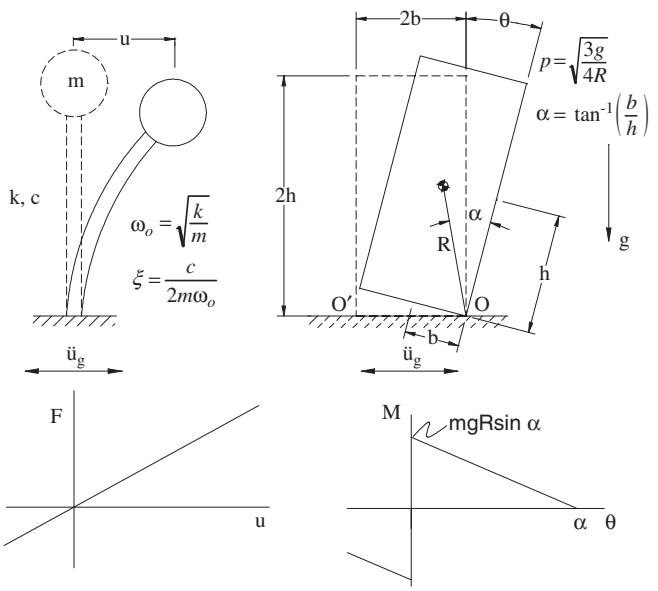

Figure 1. Schematic of a single-degree-of-freedom oscillator (top left) and of a free-standing block in rocking motion (top right); together with the associated force–displacement (bottom left) and moment-rotation (bottom right) diagrams.

loss will induce a lift that distorts the pure rocking assumption. The finite energy loss during impact results in an instantaneous reduction of the angular velocity when the rotation reverses—therefore, in theory, the angular velocity history is non-differentiable. In reality, during impact, there is a local plastic deformation at the pivot point that results in large but finite angular accelerations, which are not computed in this analysis. Regardless of what the exact value of the angular acceleration is, the existence of rocking motion is inherently associated with damping. Hence the rocking response of a rigid block is compared with the oscillatory response of a *damped oscillator*. In this study we focus on the viscously damped oscillator, although other damping mechanisms could be assumed without difficulty. Within the context of constitutive relations, the restoring mechanism of the SDOF oscillator originates from the elasticity of the structure, while the restoring mechanism of the rocking block originates from gravity. Figure 1 (bottom) shows the force–displacement and moment–rotation relations of the two elementary structures of interest. Some of the fundamental differences in the mechanical structure of these two systems become apparent. The SDOF oscillator has a positive and finite stiffness, k, and energy is dissipated as the force–displacement curve forms closed loops. In contrast, the rocking block has infinite stiffness until the magnitude of the applied moment reaches $mgR\sin\alpha$, and once the block is rocking, its stiffness assumes a negative value and decreases monotonically, reaching zero when $\theta = \alpha =$ block slenderness.

REVIEW OF THE EARTHQUAKE RESPONSE OF THE TWO OSCILLATORS

Regular pendulum

Dynamic equilibrium of the mass m of the SDOF oscillator with stiffness, k and damping, c shown at the top left of Figure 1 gives

$$\ddot{u}(t) + 2\xi\omega_0\dot{u}(t) + \omega_0^2 u(t) = -\ddot{u}_g(t) \tag{1}$$

where, $\xi = c/2m\omega_0$ is the viscous damping ratio, $\omega_0 = \sqrt{k/m}$ is the undamped natural frequency, and $\ddot{u}_g$ is the ground-induced horizontal acceleration. Equation (1), and its solution have been treated in several books of structural dynamics [10, 11]. Traditionally, the earthquake response of the SDOF oscillator has been presented in terms of response maxima as a function of the fundamental period of the oscillator, $T_o = 2\pi/\omega_0$, and the viscous damping ratio, ξ.

Figure 2 (left) plots the true displacement, velocity, and acceleration spectra of the linear, viscously damped oscillator for values of damping $\xi = 5$, 10, and 15%, subjected to the fault–normal component of the Pacoima Dam motion recorded during the 1971 San Fernando earthquake. The bottom-left graph also shows the $\xi = 5\%$ UBC97 [12] (type-D soil is assumed for all UBC spectra in this report) and FEMA 356 [9] acceleration design spectra tailored for the specific site. Table I shows the parameters used to construct the FEMA 356 design acceleration spectra for the U.S. ground motions appearing in this study. The reference acceleration values of S_{xs} and S_{x1} that define the shape of the design spectrum are obtained by modifying the mapped S_s and S_1 values for the appropriate site class. The FEMA design displacement spectra shown in the top-left graphs of Figures 2, 3, 6, and 8–11, are computed with the design formula

$$S_d = S_a g \frac{T_o^2}{4\pi^2} \tag{2}$$

as recommended in Chapter 4, *Foundations and Geologic Site Hazards*, of the FEMA 356 document [9]. Clearly, the spectral displacement values resulting from Equation (2) do not converge at long periods to the actual peak ground displacements. In contrast, the true displacement spectra shown in the top left of Figure 2 initially increase with the structural period and eventually converge to the peak ground displacement. Similar trends are observed in Figures 3, 6, and 8–11, that plot true response spectra for other major historic earthquakes.

Inverted pendulum

We consider the rigid block shown on the right of Figure 1. The block can pivot about the centres of rotation O and O' when it is set to rocking. Depending on the level and form of the ground acceleration, the block may translate with the ground, slide, rock, or slide-rock. Before 1996, the mode of rigid body motion that prevailed was determined by comparing the available static friction to the width-to-height ratio of the block, irrespective of the magnitude of the horizontal ground acceleration. Shenton [5] indicated that in addition to pure sliding and pure rocking, there is a slide-rock mode, and its manifestation depends not only on the width-to-height ratio and the static friction coefficient, but also on the magnitude of the base acceleration.

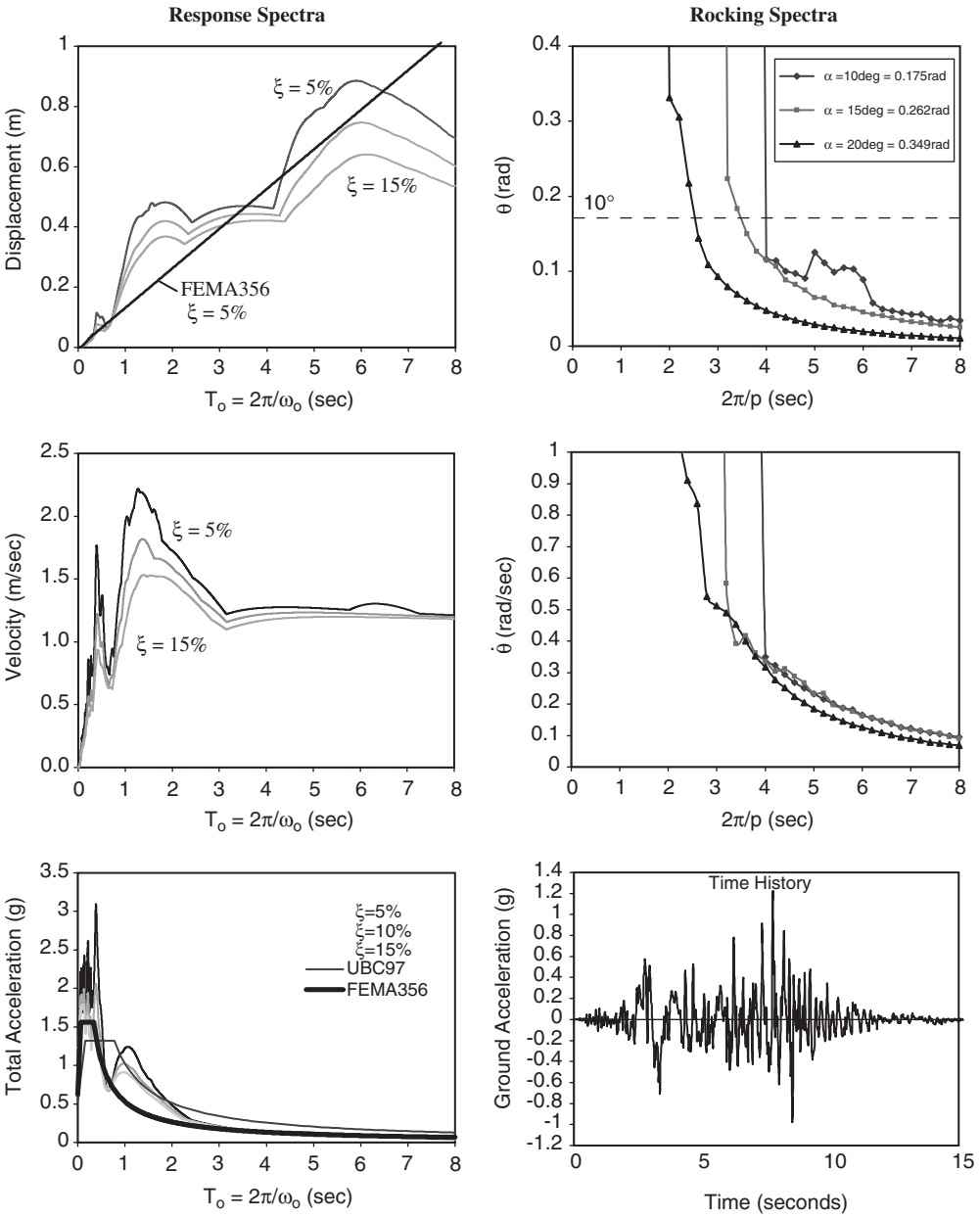

Figure 2. True response spectra of a linear viscously damped oscillator (left) and rocking spectra of a rigid slender block (right) when subjected to the Pacoima Dam motion recorded during the 1971 San Fernando Earthquake.

Table I. Parameters used to construct the FEMA design acceleration spectra.

Earthquake	Ground motion	Site class	S_{xs} (g)	S_{x1} (g)
San Fernando (1971)	Pacoima Dam	B	1.59	0.5
Imperial Valley (1979)	El Centro #5	D	1.34	0.81
Loma Prieta (1989)	Los Gatos	D	1.94	1.83
Northridge (1994)	Rinaldi FN	C	1.56	0.69
Northridge, 1994	Sylmar FN	D	1.56	0.8

Assuming that the coefficient of friction is large enough so that there is no sliding, under a positive horizontal acceleration that is sufficiently large, a rigid block will initially rotate with a negative rotation, $\theta<0$, and, if it does not overturn, it will eventually assume a positive rotation; and so on.

The equation that governs the rocking motion under a horizontal ground acceleration $\ddot{u}_g(t)$ is

$$\ddot{\theta}(t)=-p^2\left\{\sin[\alpha\,\mathrm{sgn}[\theta(t)]-\theta(t)]+\frac{\ddot{u}_g}{g}\cos[\alpha\,\mathrm{sgn}[\theta(t)]-\theta(t)]\right\} \tag{3}$$

where p is the *frequency parameter* of the block. For a rectangular block, $p=\sqrt{3g/4R}$. The larger the block (larger R), the smaller p. Equation (3) is well known in the literature [6, 7] and is valid for arbitrary values of the angle $\alpha=\tan^{-1}(b/h)$. The solution of Equation (3) is obtained numerically via a state-space formulation [6, 7] with standard ODE solvers available in MATLAB [13]. The solution is constructed by accounting for the energy loss at every impact. When the angle of rotation reverses, it is assumed that the rotation continues smoothly from point O to O'. Conservation of angular momentum about point O' just before the impact and immediately after the impact gives the maximum value of the coefficient of restitution $e=\sqrt{r}$ under which a block with slenderness α will undergo rocking motion [2],

$$e=\sqrt{r}=[1-\tfrac{3}{2}\sin^2(\alpha)] \tag{4}$$

Consequently, in order to observe rocking motion, the impact has to be inelastic. The less slender a block (larger α), the more energy has to be lost during impact in order to observe rocking motion. Therefore, the slenderness of a rocking block is a measure of the minimum damping of the system.

The integration of (3) in conjunction with the constraint imposed by (4) yields time histories of the rotation and angular velocities. Figure 4 shows the computed rotation and angular velocity histories of a rigid block with frequency parameter $p=2.0$ rad/s ($2\pi/p=3.14$ s) and slenderness $\alpha=15°$[$h=1.78$ m(70"), $b=0.48$ m (18.76"), $r=0.81$] subjected to three different levels of a 2-s-long one-cosine (Type-B) pulse [6],

$$\ddot{u}_g(t)=a_p\cos(\omega_p t),\quad 0\leqslant t\leqslant T_p \tag{5}$$

where $T_p=2\pi/\omega_p$ is the period and duration of the pulse. The left column of Figure 4 shows the block response when $a_p=0.310g$. Following the expiration of the pulse, the block experiences more than 20 impacts within the 8 subsequent seconds. The centre column of Figure 4 shows the block response on the verge of overturning. Note that just a 1.6% increase in the

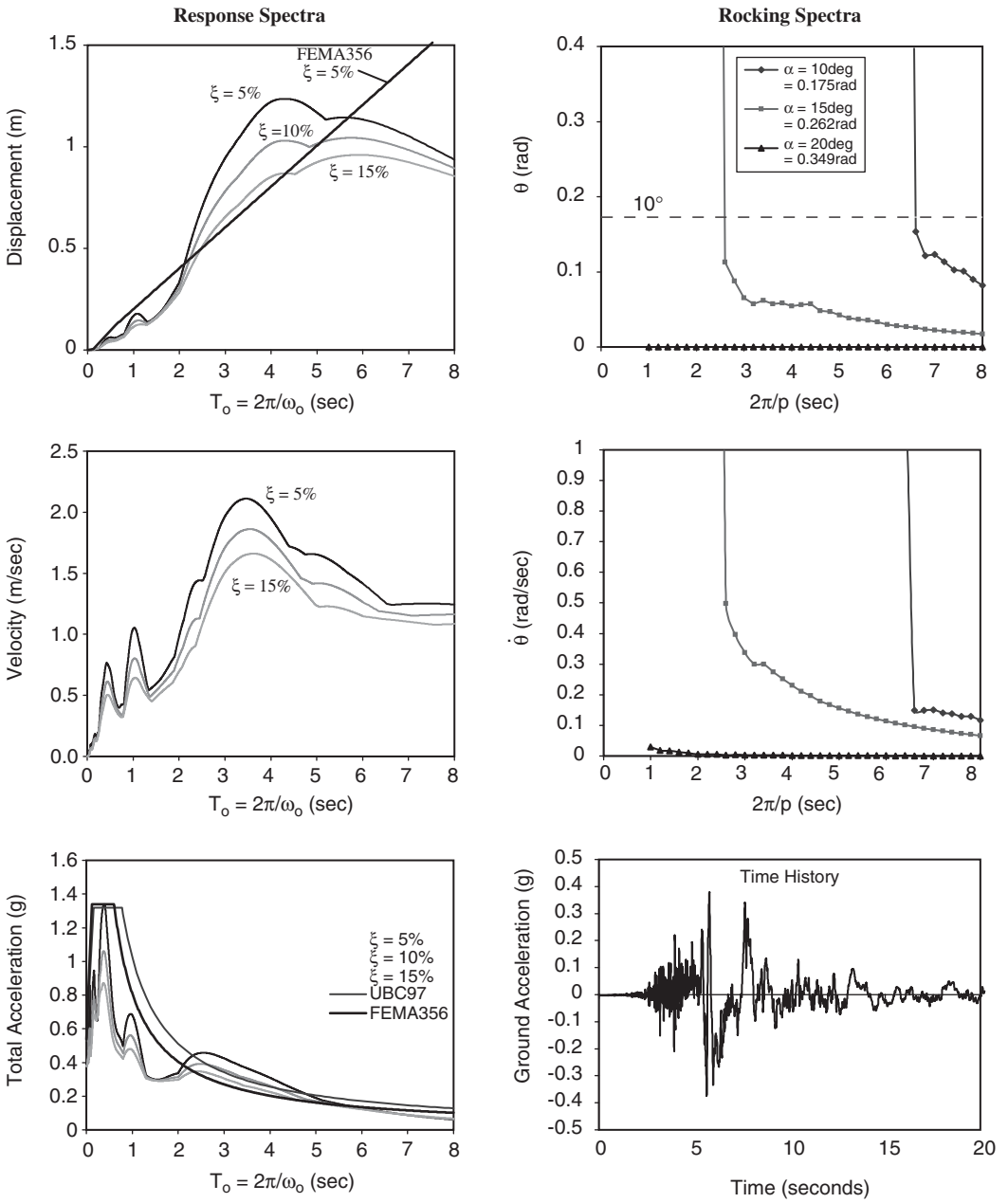

Figure 3. True response spectra of a linear viscously damped oscillator (left) and rocking spectra of a rigid slender block (right) when subjected to the FN component of the Array #5 motion recorded during the 1979 Imperial Valley earthquake.

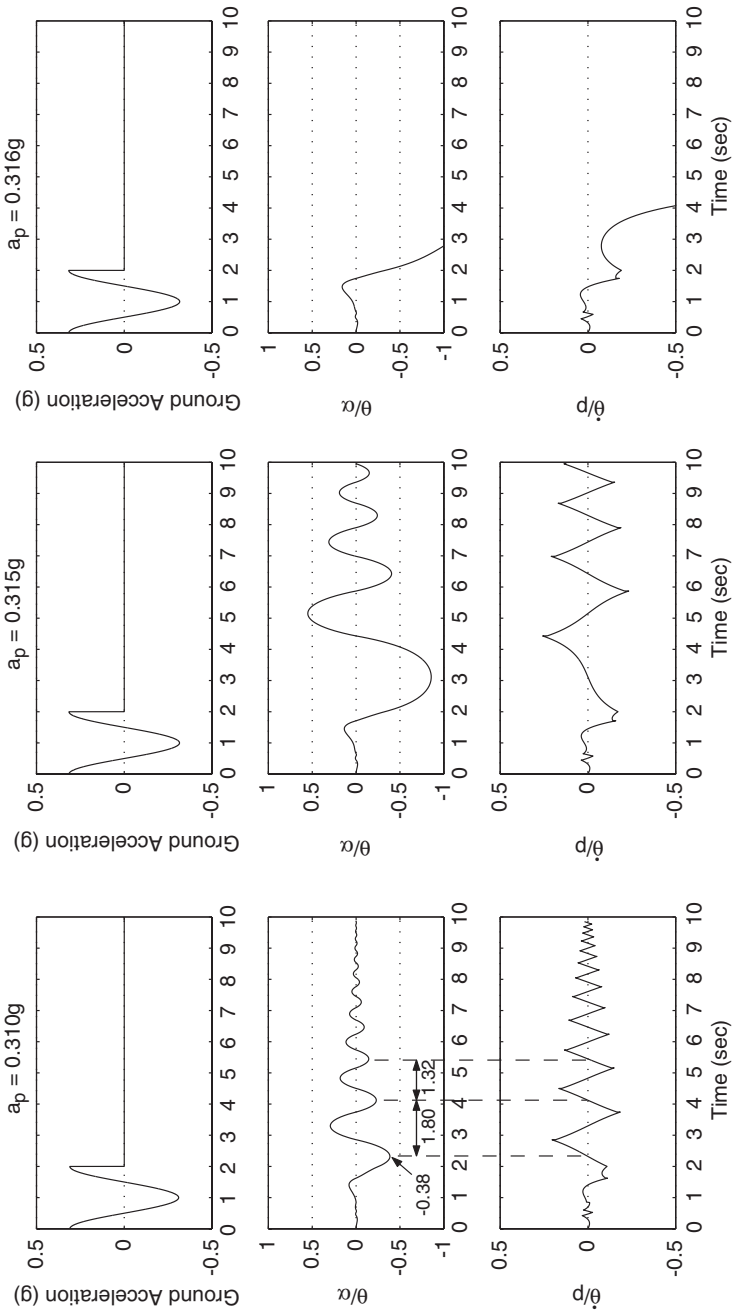

Figure 4. Rocking response of rigid block: $p=2.0$ rad/s, $\alpha=15^\circ$ [$h=1.77$ m, $b=0.48$ m, $R=1.84$ m, $r=0.81$], subjected to Type-B pulse with $T_p=2$ s.

Table II. Peak ground accelerations (PGA), peak ground velocities (PGV) and approximate main pulse periods of selected earthquake motions next to values of block-slenderness of interest.

Ground motion	PGA/g	PGV (m/s)	Approximate value of main pulse period, T_p (s)	Slenderness α	$\tan(\alpha)$
San Fernando (1971) Pacoima Dam	1.226	1.2	1.3	$10^\circ = 0.175$ rad	0.176
Imperial Valley (1979) El Centro #5	0.379	0.9	3.2	$12^\circ = 0.209$ rad	0.212
Loma Prieta (1989) Los Gatos	0.563	0.95	3	$15^\circ = 0.262$ rad	0.268
Northridge (1994) Rinaldi FN	0.838	1.75	1	$17^\circ = 0.297$ rad	0.306
Northridge (1994) Sylmar FN	0.732	1.2	2.3	$20^\circ = 0.349$ rad	0.364

acceleration amplitude of the excitation pulse alters drastically the response that exhibits only 7 impacts within the subsequent 8 s. The right column of Figure 4 shows the block response when it overturns, which happens for an acceleration amplitude $a_p = 0.316g$. Note that when the block does not overturn (left and centre columns), the frequency of vibration during the free-vibration regime increases as the rotation amplitude decreases.

ROCKING SPECTRA

Parallel to the response spectra, one can generate rotation and angular velocity spectra (rocking spectra) as a function of the 'period' $T = 2\pi/p$ and different values of slenderness (damping), $\alpha = \tan^{-1}(b/h)$. The minimum ground acceleration needed to initiate rocking can be computed from static analysis, which yields that $\ddot{u}_g/g \geqslant \tan(\alpha)$. Table II offers the peak ground acceleration (PGA) of the strong-motion records used in this study together with the values of $\tan(\alpha)$ for the range of slenderness that is of interest. For instance, the El Centro Array #5 record with PGA/$g = 0.379$ can barely induce uplift to a block with slenderness $\alpha = 20^\circ$ ($\tan(\alpha) = 0.364$); however, it will not be able to uplift a block with $\alpha = 21^\circ$ since $\tan(21^\circ) = 0.384 > 0.379 = \text{PGA}/g$. Next to the peak ground accelerations, Table II offers the peak ground velocities of the ground motions together with the duration of main pulses that can be identified within most of these main near-source ground motions [6]. These kinematic characteristics of the ground are used later in this section where observations from response spectra and rocking spectra are discussed.

The right side of Figures 2 and 3 plots rotation and angular velocity spectra next to the displacement and velocity spectra presented earlier. As $2\pi/p$ increases, one moves to larger blocks. Larger values of the slenderness α correspond to larger amount of energy lost during impact. The most striking observation is that the displacements of oscillating structures, increase as the natural period $T_o = 2\pi/\omega_0$ increases, reach a maximum, and subsequently

Table III. Selective characteristics and parameters of the two one-degree-of-freedom systems of interest.

Parameters/ characteristics	Damped oscillator m, c, k	Rocking rigid block b, h, g
Restoring mechanism	Elasticity of the structure	Gravity
Restoring force/moment	$F = ku$ (*for linear springs*)	$M = mgR\sin(\alpha - \theta)$ $R = \sqrt{b^2 + h^2}$
Stiffness at stable equilibrium	Finite	Infinite
Restoring force/moment at stable equilibrium	Zero	Finite: $mgR\sin(\alpha)$
Stiffness away from equilibrium	Positive	Negative
Frequency parameter	Undamped natural frequency: $\omega_0 = \frac{2\pi}{T_o} = \sqrt{\frac{k}{m}}$	Frequency parameter: $p = \sqrt{\frac{3g}{4R}}$ (*for rectangular blocks*)
Damping parameter	Viscous damping ratio: $\xi = \frac{c}{2m\omega_0}$	Slenderness: $\alpha = \tan^{-1}(b/h)$

converge to the ground displacement; whereas the rotations of rocking structures decrease nearly monotonically as their apparent 'period' $T = 2\pi/p$ increases. In addition to the different trends observed in the spectra of the SDOF oscillator and the rocking block, Table III summarizes selective characteristics and parameters that emerge from the two systems of interest and identifies some of the fundamental differences in their dynamical structure. In view of these inherent differences, any analogy between the responses of the two systems tends to be superficial.

Before examining the shortcomings that result from the superficial analogy between the response of a SDOF structure and a rocking block, this section elaborates on some interesting observations which indicate that the rocking spectra can be used as a supplemental measure of earthquake intensity which complements the valuable information that one draws from the response spectra. Figure 2 (right) indicates that any block with slenderness $\alpha = 10°$ that is small enough so that $2\pi/p < 4$ [$R < 2.98$ m (117.3")] will overturn when subjected to the Pacoima Dam record. Less slender blocks experience smaller rotations and are in principle more stable. For instance, a block with slenderness $\alpha = 20°$ will survive the Pacoima Dam record even if it is as small as $2\pi/p = 2$ [$R = 0.74$m (29.3")]. Larger blocks, say $2\pi/p > 6$ [$R > 6.71$m (264.0")], will uplift, but the maximum rotation is only a fraction of their slenderness α even for the strong ground motions with PGA/g more than four times the slenderness of a block with $\alpha = 15°$ (See Table II).

Figure 3 (right) shows rocking spectra from the fault–normal component of the Array #5 motion recorded during the 1979 Imperial Valley earthquake that has a PGA/g 0.379, which is slightly larger than the value of $\tan(20°) = 0.364$. The rotations induced by the Array #5 record to blocks with slenderness $\alpha = 15°$ are comparable to the rotations induced to the same

blocks by the Pacoima Dam record; smaller blocks ($2.6 \leqslant 2\pi/p \leqslant 3$) survive the more 'gentle' Array #5 record yet topple due to the more 'violent; Pacoima Dam record. When observing the response of blocks with slenderness $\alpha = 10°$, the situation reverses. The Array #5 record topples every block with $2\pi/p < 6.5$ whereas blocks with $\alpha = 10°$ are much more stable when subjected to the Pacoima Dam record, as every block with $2\pi/p > 4$ survives the motion. The reason that the Array #5 record is more capable than the Pacoima Dam record to overturn slender blocks is because it contains a 3.2-s-long Type-B pulse [6]. The significance of the duration of a long pulse in achieving overturning in association with its acceleration intensity has been discussed in depth in References [6, 7].

The response spectra of the Pacoima Dam record and the Array #5 record also exhibit noticeable differences but of a different nature. For instance, up to $T_o \approx 2.0$ s, the Pacoima Dam record results in higher spectral displacements than the Array #5 record. However, at $T_o = 4$ s, the Array #5 record results in spectral displacements more than two times the spectral displacements that result from the Pacoima Dam record. Nevertheless, this behaviour is uniform for all three values of damping, $\xi = 5,\ 10$, and 15%, contrary to the case of rocking spectra for which the behaviour is nonuniform for different values of slenderness (damping). Additional discussion related to the nonuniformity of rocking spectra from other earthquakes is offered in Reference [15].

In conclusion, this section highlights the following two observations which uncover major differences in the trends of the response and rocking spectra:

(a) When for a prescribed value of viscous damping, a response spectrum of a given earthquake exceeds the response spectrum of another earthquake, the same will happen (with few local exceptions) for a different value of viscous damping. Contrarily, when for a prescribed slenderness, the rocking spectrum of a given earthquake exceeds the rocking spectrum of another earthquake, it is not guaranteed that the same will happen for a slightly different value of the slenderness.
(b) There are period ranges where the values of the displacement spectra are nearly insensitive to the value of viscous damping ratio ξ. However, the rotation (uplift) spectra are very sensitive to the value of slenderness α throughout the $2\pi/p$ range.

The abovementioned differences have been the main motivation for proposing the use of the rocking spectrum as a complementary tool to the response spectrum in order to quantify the shaking potential of a ground motion.

FREE VIBRATIONS OF ROCKING BLOCK

The rocking motion of a rigid block is an inherently non-linear problem. Non-linearities emerge from several sources and become dominant when the rotation of the block, θ, approaches or exceeds its slenderness α. For instance, it has been recently shown [7, 14] that the overturning of a rigid block is a *multivalued* problem since a rigid block can survive a ground acceleration that exceeds the first ground acceleration which is capable of overturning it. This multivalued and non-linear response exists even for very slender blocks, and the above mentioned references have shown that there is a frequency range where Equation (3) cannot be linearized even for small values of the slenderness α.

During a free-vibration regime that does not result in toppling (say with initial conditions $\theta_0 < \alpha$ and $\dot{\theta}_0 = 0$), the situation is simpler than during a forced vibration regime, and the equations of rocking motion can be linearized with confidence for slender blocks (say $\alpha \leqslant 20^\circ$) [2].

The free-vibration response of the rocking block at its linear limit was investigated by Housner [2], who was able to derive a relation between the maximum rotation, θ_n, after the nth impact, and the initial rotation, θ_0,

$$\frac{\theta_n}{\alpha} = 1 - \sqrt{1 - r^n \left[1 - \left(1 - \frac{\theta_0}{\alpha}\right)^2\right]} \tag{6}$$

where $r = e^2$ is given by (4). Equation (6) that relates the rotation after $m = n/2$ cycles to the initial rotation θ_0, stimulates the temptation to relate its result with the so-called logarithmic decrement of the amplitude of the mth cycle of a SDOF damped oscillator

$$\ln\left(\frac{u_o}{u_m}\right) = \frac{2m\pi\xi}{\sqrt{1-\xi^2}} \tag{7}$$

Equation (7) for lightly damped systems becomes

$$\xi = \frac{1}{2m\pi} \ln\left(\frac{u_o}{u_m}\right) \tag{8}$$

after approximating $\sqrt{1-\xi^2}$ with one.

Priestley *et al.* [8] noticed this resemblance—while downplayed the fundamental differences in the mathematical structure of the response of the two systems (see Table III)—and proposed that since there is an apparent correspondence between the displacement u of a SDOF oscillator and the rotation θ of a rocking block, one can define an equivalent viscous damping ratio for the rocking block

$$\beta = \frac{1}{n\pi} \ln\left(\frac{\theta_0}{\theta_n}\right) \tag{9}$$

since in m cycles the block has experienced $n = 2m$ impacts (see free-vibration response in Figure 4 that happens after the expiration of the Type-B pulse). Substituting Equation (6) into Equation (9) gives

$$\beta = \frac{1}{n\pi} \ln\left\{\frac{\theta_0}{\alpha}\left[1 - \sqrt{1 - r^n\left[1 - \left(1 - \frac{\theta_0}{\alpha}\right)^2\right]}\right]^{-1}\right\} \tag{10}$$

Figure 5 plots the relation between the equivalent viscous damping ratio, β, and r as results from Equation (10) for values of initial rotation $\theta_0/\alpha = 0.1$ to 0.7 and for four values of the number of impacts, $n = 2$, 4, 6, and 8. As Priestley *et al.* indicated, this relation is comparatively insensitive to the initial rotation, θ_0/α, and number of impacts, n, and an average relation between β and r can be proposed that is independent of θ_0/α and n. An empirical equation that approximates this relation is

$$\beta = -0.34 \ln(r) \tag{11}$$

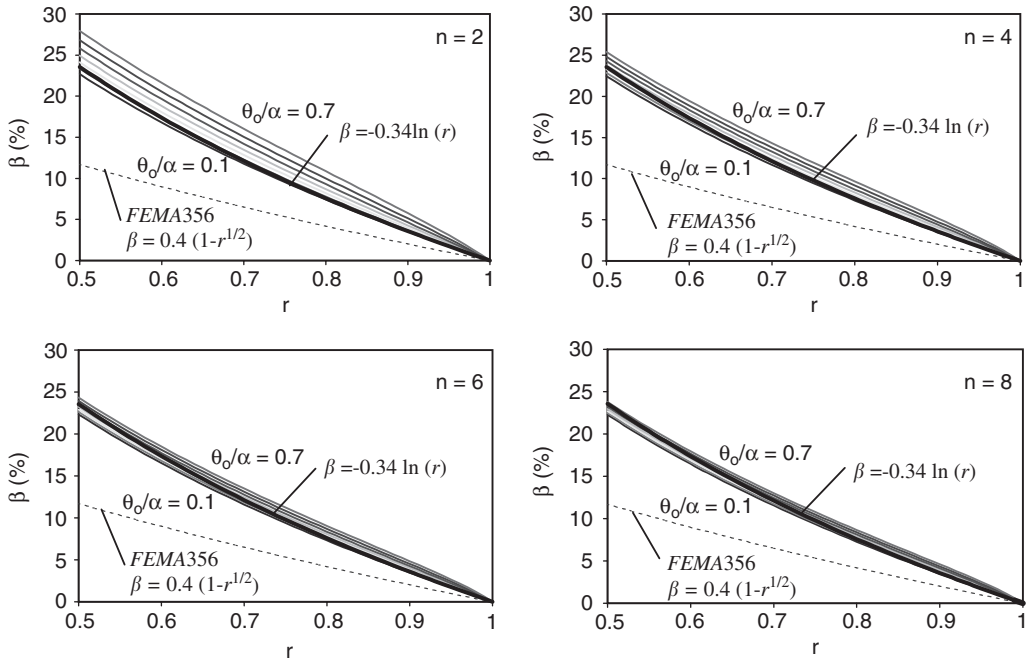

Figure 5. Equivalent viscous damping, β, of a rocking block as results from (a) the Priestley *et al.* [8] analogy (Equation (10)), (light solid lines); (b) the empirical Equation (11), (heavy solid lines); and (c) the FEMA 356 formula, (dashed lines).

and its performance is shown with a heavy line in each quarter of Figure 5. The results of Equation (11) are very close to the graphical relation shown in Figure 3 of the Priestley *et al.* paper which indicates that values of the equivalent viscous damping ratio β will vary from this relationship by less than 10% for values of $\theta_0/\alpha \leqslant 0.5$ for $n \leqslant 16$. While the Priestly *et al.* reasoning and the results shown in Figure 5 appear reasonable to the nonspecialist engineer, attention is redirected to Figure 4 that illustrates the divergent nature of the hyperbolic functions appearing in the free-vibration response of the rocking block [2, 6, 7]. The left column of Figure 4 plots the rocking response when the acceleration amplitude of the 2-s-long cosine pulse is $0.310g$. Note that after the excitation pulse expires ($t=2$ s), the block experiences a negative rotation that reaches a maximum of $\theta/\alpha=0.38$ and subsequently the block vibrations decay. A slightly stronger excitation, $a_p=0.315g$ induces a much more pronounced negative rotation that reaches a maximum of $\theta/\alpha=0.86$. Therefore, a 1.6% change in the excitation amplitude results in approximately 125% change in the response. A minor further increase in the input results in overturning (catastrophe). In contrast to the response shown in Figure 4, the oscillatory response of a SDOF oscillator with $\omega_0=p=2$ rad/s and $\xi=-0.34\ln(r)=7.2\%$ (where r corresponds to $\alpha=15^\circ$) is insensitive to small variations of the acceleration level of a Type-B pulse [15].

ESTIMATION OF UPLIFT USING THE RESPONSE SPECTRA

The availability of design response spectra in association with observations from strong earthquakes motivated Priestley *et al.* [8] to propose a relatively simple procedure to estimate structural displacements that originate from rocking (uplift). It includes the following steps:

(i) Establish that the ground acceleration is strong enough to induce rocking.
(ii) Using Equation (10) or the graphs of Figure 5, estimate the equivalent viscous damping ratio, $\xi=\beta$, of the rocking structure.
(iii) Estimate an initial rotation θ_i and compute the amplitude-dependent period of the rocking block from the formula derived by Housner [2],

$$T(\theta_i)=\frac{4}{p}\cosh^{-1}\left[\left(1-\frac{\theta_i}{\alpha}\right)^{-1}\right] \tag{12}$$

(iv) From a displacement response spectrum (or even a displacement design spectrum) constructed for the value of the equivalent damping ratio estimated in step (ii), read the displacement, δ_i, of the equivalent SDOF oscillator with period $T(\theta_i)$.
(v) Compute the value of the new rotation,

$$\theta_{i+1}=\frac{\delta_i}{R\cos(\alpha)} \tag{13}$$

(vi) Compute the new local period $T(\theta_{i+1})$ with Equation (12) and repeat steps (iv) and (v) until convergence is reached.

In this section, the abovementioned procedure is examined by comparing the converged values of the rotations θ that result from the Priestley *et al.* design approach with the exact rocking spectra presented in this paper. We concentrate on blocks with slenderness $\alpha=10$, 15, and 20°. For these values, the equivalent viscous damping ratios according to Equation (11) are $\beta=\xi=3.15$, 7.20, and 13.12%. Figures 6 and 8–11 (left columns), plot the response spectra of the five earthquakes used in this paper for the aforementioned values of viscous damping. The true displacement spectra shown in Figures 6 and 8–11 are used to construct the uplift spectra for blocks with $\alpha=10$, $\alpha=15$, and $\alpha=20°$, according to the Priestley *et al.* [8] approximate method. These uplift spectra are shown in the centre column of the figures together with the exact rotation spectra. In addition to the exact spectra that one computes for the 100% level of the earthquake record, the centre columns of the figures show the exact rotation spectra that one computes for the 90% level and for the 110% level of the earthquake record. This parametric study was conducted in order to assess the sensitivity of the rocking response to slight variations of the acceleration level. The evaluation of the Priestley *et al.* method is conducted by considering these variations. The third column of Figures 6 and 8–11 plots the values of the period $T(\theta)$ given from Equation (12) when evaluated with the converged values of the rotations shown in the centre plots.

The centre plot of Figure 6 indicates that for the Pacoima Dam record, the Priestley *et al.* [8] method is invariably overconservative since: (a) it predicts overturning of smaller blocks that in reality survive the Pacoima Dam record; and (b) it predicts substantially larger rotations for larger and less slender blocks. As an example, a typical electrical transformer has a frequency parameter $p \approx 2$ rad/s and a slenderness of $\alpha=20°$. According to

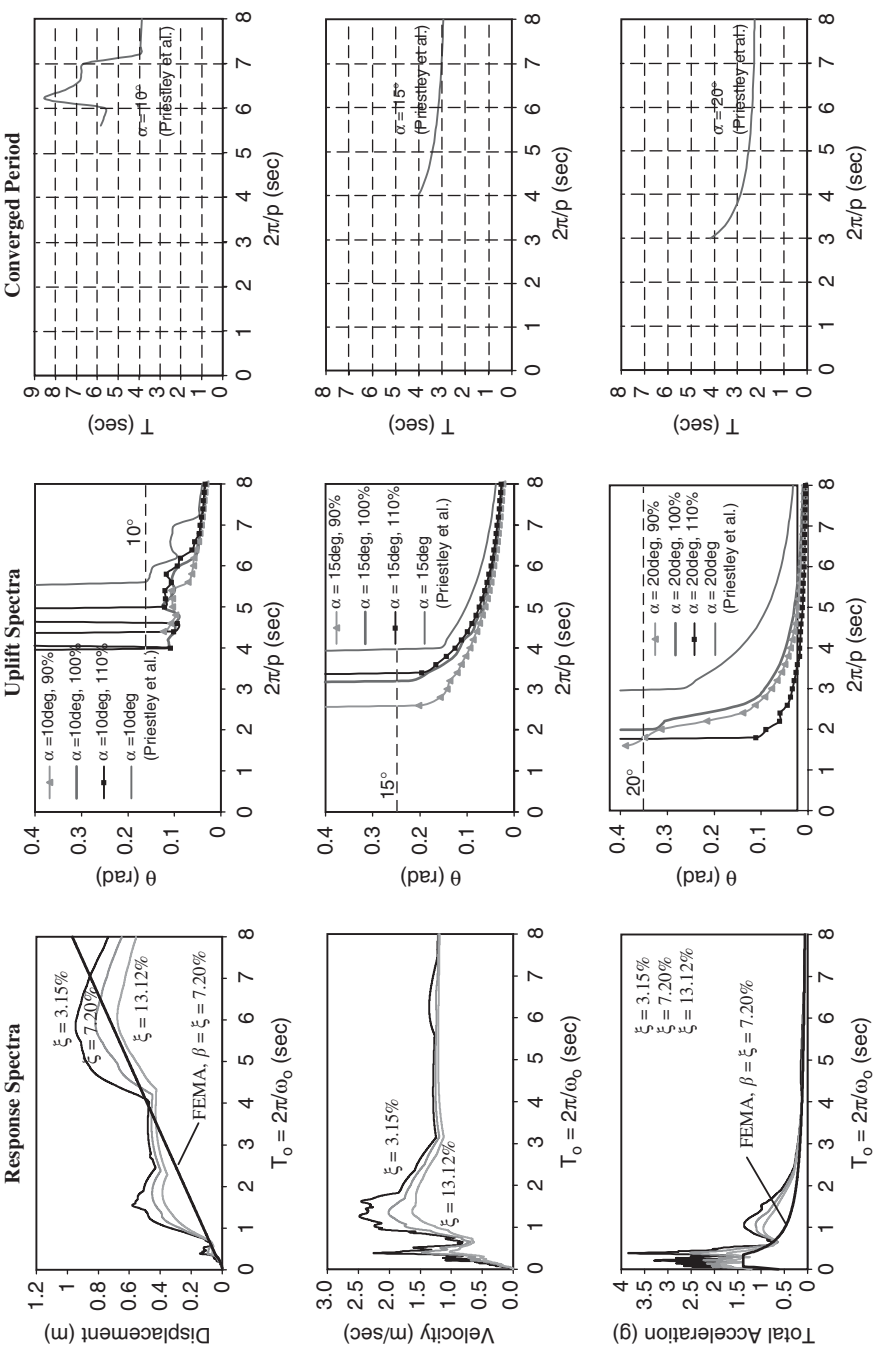

Figure 6. Comparison of exact and approximate uplift spectra (centre column) that have been computed with the Priestley *et al.* [8] method using the true displacement response spectrum (top left). The converged period that corresponds to the estimated uplift is shown in the right column. Ground Motion: Pacoima Dam, 1971 San Fernando.

the bottom–centre plot, the approximate method predicts a rotation of $\theta=0.25$ rad whereas the exact solution gives $\theta=0.08$ rad—that is less than three times smaller. As $2\pi/p$ increases, the predictions of the Priestley *et al.* method become more dependable, in particular for slender blocks. Concentrating on the top-right graph of Figure 6, the approximate method indicates that for $2\pi/p=6$ s and $\alpha=10°$, the converged period of rocking is approximately $T(\theta)=5.7$ s whereas for $2\pi/p=7$ s, the converged period of rocking is $T(\theta)=6.6$ s. Figure 7 (left) plots the exact time histories of blocks with size $2\pi/p=6$ s (centre left) and $2\pi/p=7$ s (bottom left) and slenderness $\alpha=10°$. The rocking cycles have different durations, but the general trend is that larger blocks experience smaller rotations with the corresponding cycles having smaller durations. For $2\pi/p=6$ s ($R=6.71$ m), the maximum duration of one cycle is 5.25 s, which is indeed close to the period estimated by the approximate method ($T(\theta)=5.7$ s). For $2\pi/p=7$ s ($R=9.12$ m), the maximum duration of one cycle is 3.61 s that is considerably smaller than the period estimated by the approximate method ($T(\theta)=6.6$ s).

The Priestley *et al.* method is flawed because it attempts to compute rotations $\theta(T)=\delta(T_o)/(R\cos(\alpha))$ by reading the $\delta(T_o)$ values from the displacement spectrum that shows a behaviour totally different than that of the rotation spectrum. The fact that Equation (12) converges to some value as $\delta(T_o)$ gets updated has nothing to do with the actual duration of the rocking cycles. For instance, for $2\pi/p=7$ s and $\alpha=20°$, the converged period shown in Figure 6 is approximately $T(\theta)=2.28$ s whereas the maximum duration of one cycle from the exact time history is 1.38 s. According to the bottom-centre plot, the approximate method predicts a rotation of 0.05 rad whereas the exact solution gives $\theta=0.015$ rad.

Now, the reason that the approximate spectrum assumes decreasing values as $2\pi/p$ increases is that a nearly constant spectral displacement (see values of spectral displacement in the vicinity of $T_o=3$ s) is divided by an increasing R (see Equation (13)). This has nothing to do with the mechanism of uplifting of a free-standing rigid block.

Figure 8 indicates that for the El Centro Array #5 record, the approximate method predicts with accuracy the rotations of large blocks with $\alpha=10°$ while grossly overestimates the rotations of blocks with $\alpha=15°$ and $\alpha=20°$. A similar pattern is observed in Figure 9 which compares the rotation spectra of the Los Gatos record.

Figure 10 shows that for the Rinaldi record, the approximate method of Priestley *et al.* produces very good estimates of the rotations for all three values of $\alpha=10$, 15, and 20°. This good agreement is partly due to the unique shaking strength and morphology of the Rinaldi record. It exhibits a distinct 1-s-long acceleration pulse with amplitude that reaches $0.9g$. Because the main pulse that dominates the response has a relative short duration (around 1 s), the displacement response spectrum initiates its descent relatively early so that the trend followed by the displacement spectra beyond $T_o=4$ s resembles the trend followed by the rocking spectrum beyond $2\pi/p=4$ s. It is because of these unique yet accidental similarities between the response spectra and the rocking spectra that the Priestley *et al.* method yields such remarkably good predictions of the block rotations due to the Rinaldi motion. Selected time histories of rocking blocks and the durations of the main rocking cycles are offered in Reference [15]. All durations of the main cycles are noticeably smaller than the converged periods calculated using the approximate method.

Figure 11 shows that for the Sylmar record, the approximate method is unconservative for $\alpha=10°$ but is overconservative for $\alpha=20°$. This is true even when the rocking spectra are computed with the 110% level of the record. Additional evidence on the limitations of the Priestly *et al.* [8] methodology is offered in the report by Makris and Konstantinidis [15].

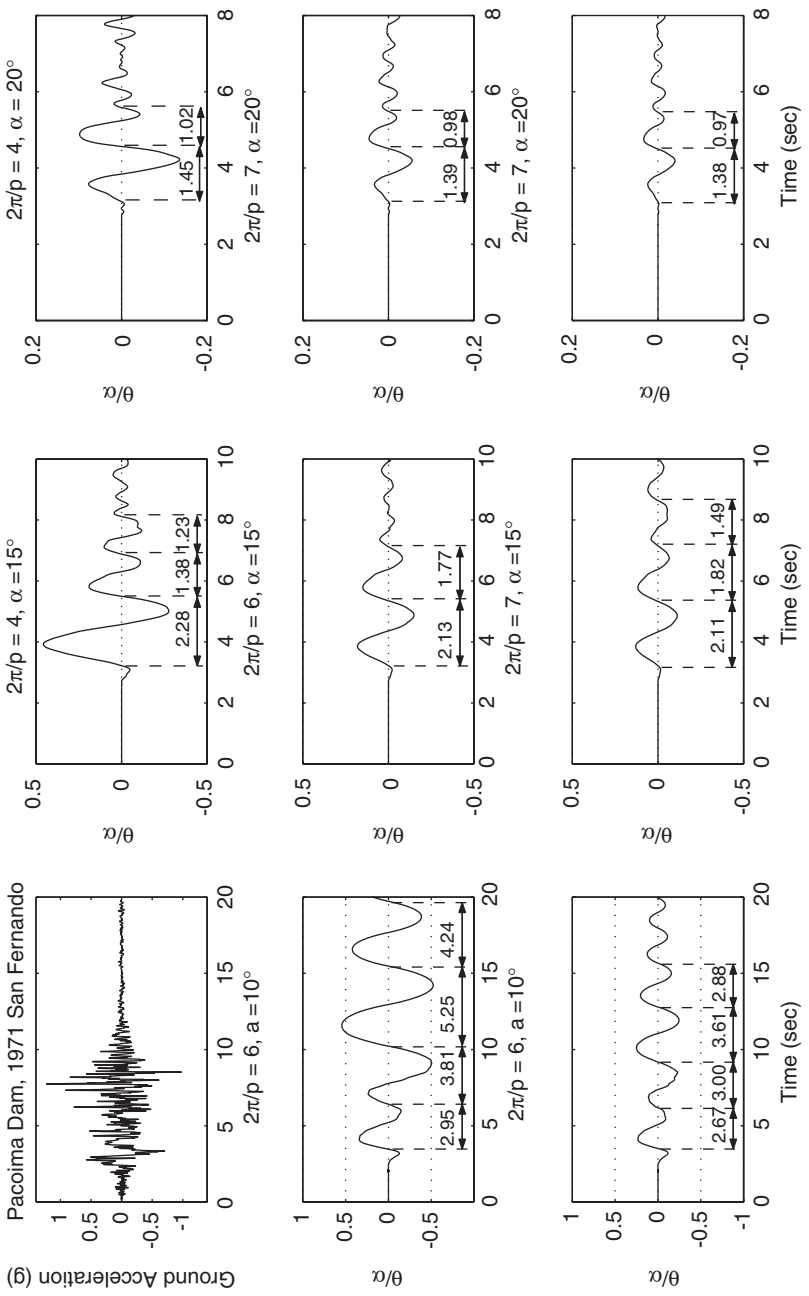

Figure 7. Selected time histories and durations of rocking cycles of rigid blocks with slenderness, $\alpha = 10°$ (left), $\alpha = 15°$ (centre), and $\alpha = 20°$ (right) when subjected to the Pacoima Dam record.

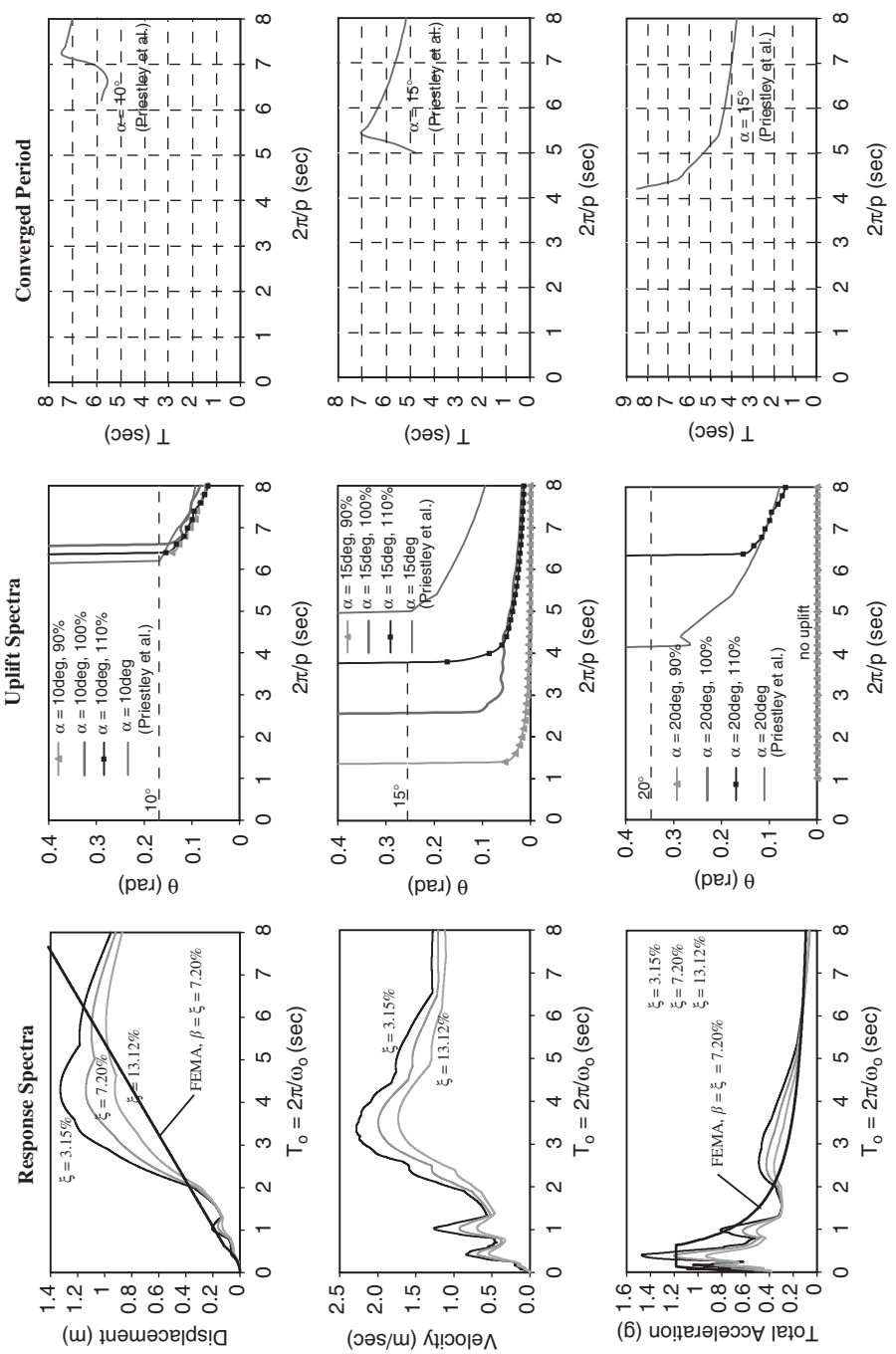

Figure 8. Comparison of exact and approximate uplift spectra (centre column) that have been computed with the Priestley *et al.* [8] method using the true displacement response spectrum (top left). The converged period that corresponds to the estimated uplift is shown in the right column. Ground Motion: El Centro Array #5, 1979 Imperial Valley.

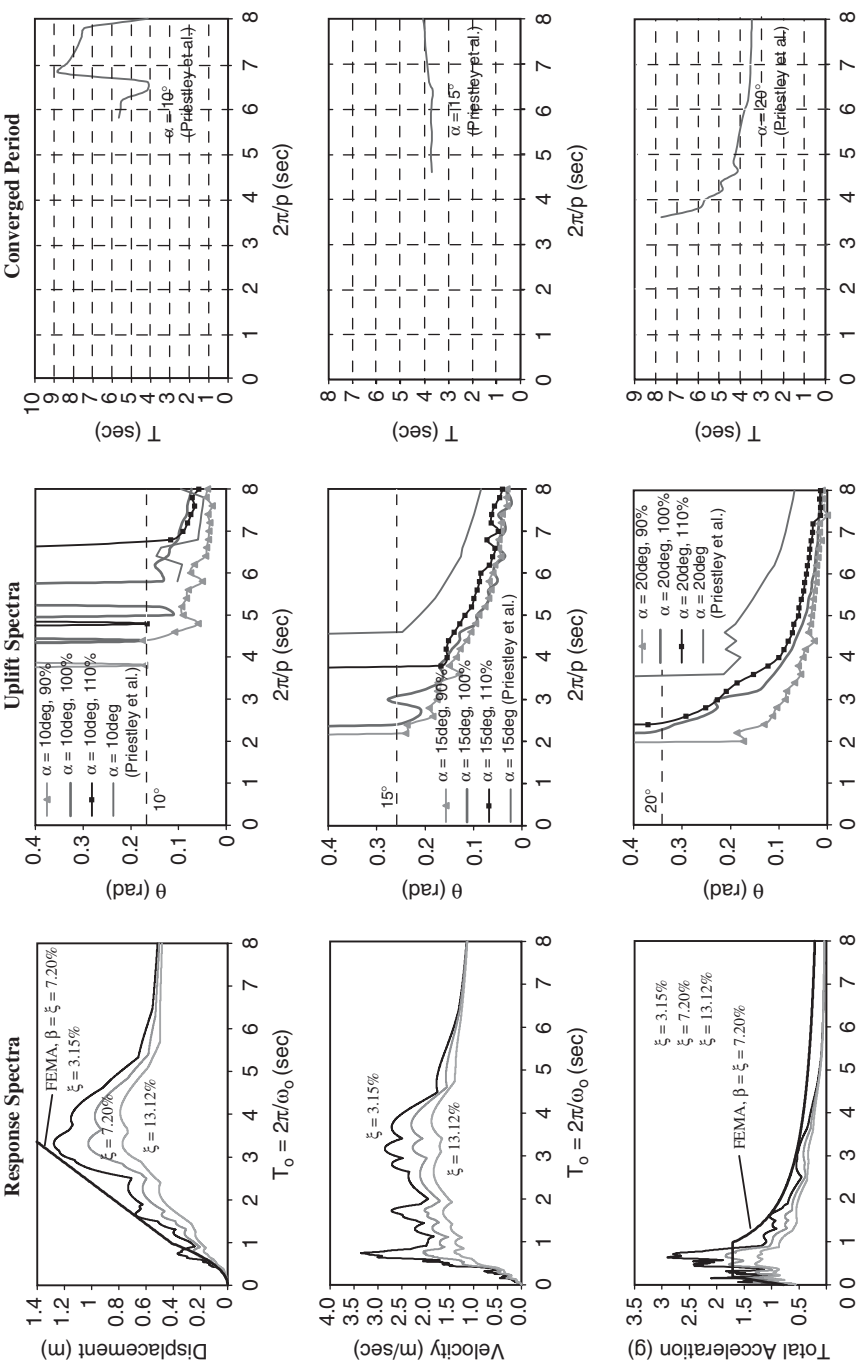

Figure 9. Comparison of exact and approximate uplift spectra (centre column) that have been computed with the Priestley *et al.* [8] method using the true displacement response spectrum (top left). The converged period that corresponds to the estimated uplift is shown in the right column. Ground Motion: Los Gatos, 1989 Loma Prieta.

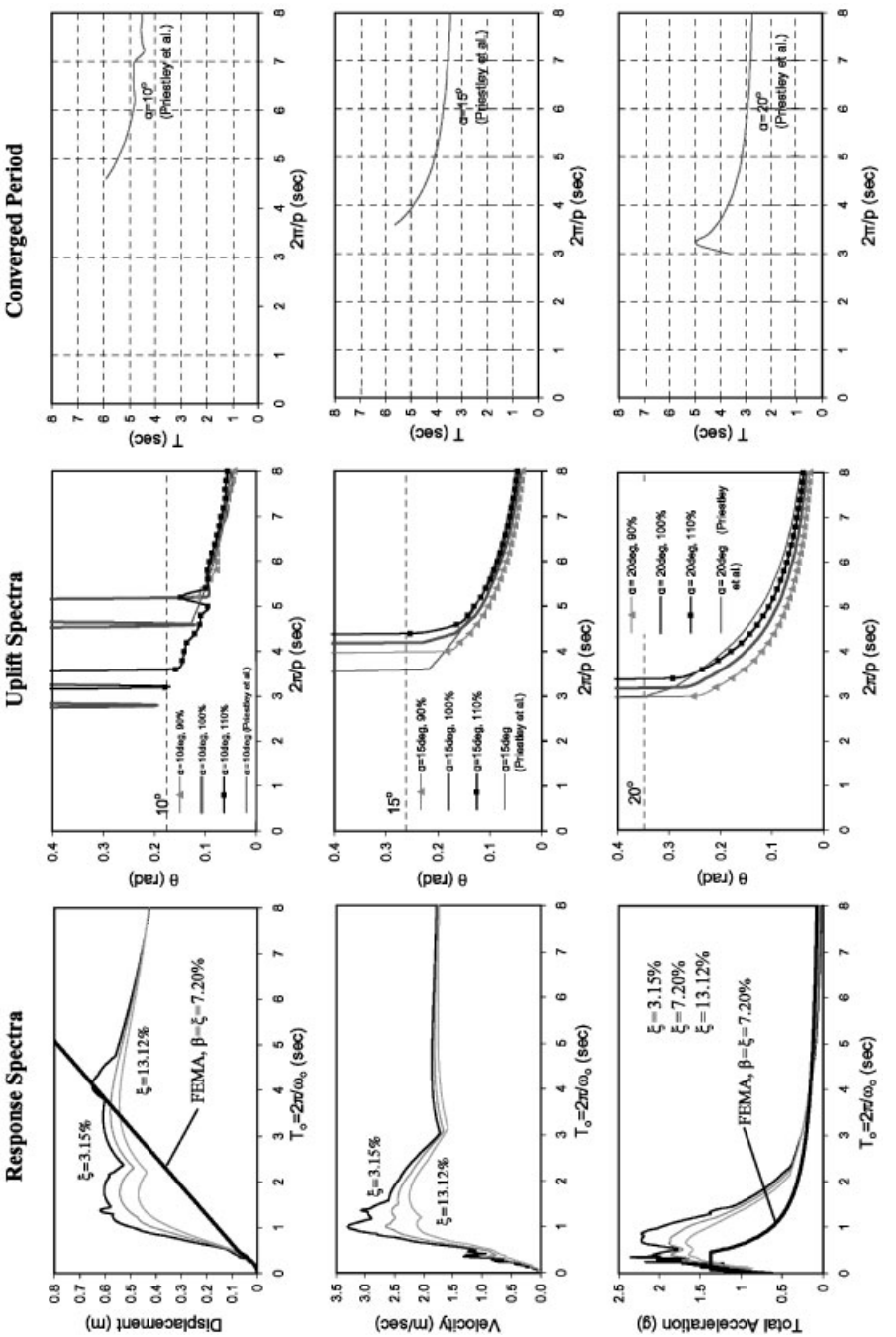

Figure 10. Comparison of exact and approximate uplift spectra (centre column) that have been computed with the Priestley *et al.* [8] method using the true displacement response spectrum (top left). The converged period that corresponds to the estimated uplift is shown in the right column. Ground Motion: Rinaldi, 1994 Northridge.

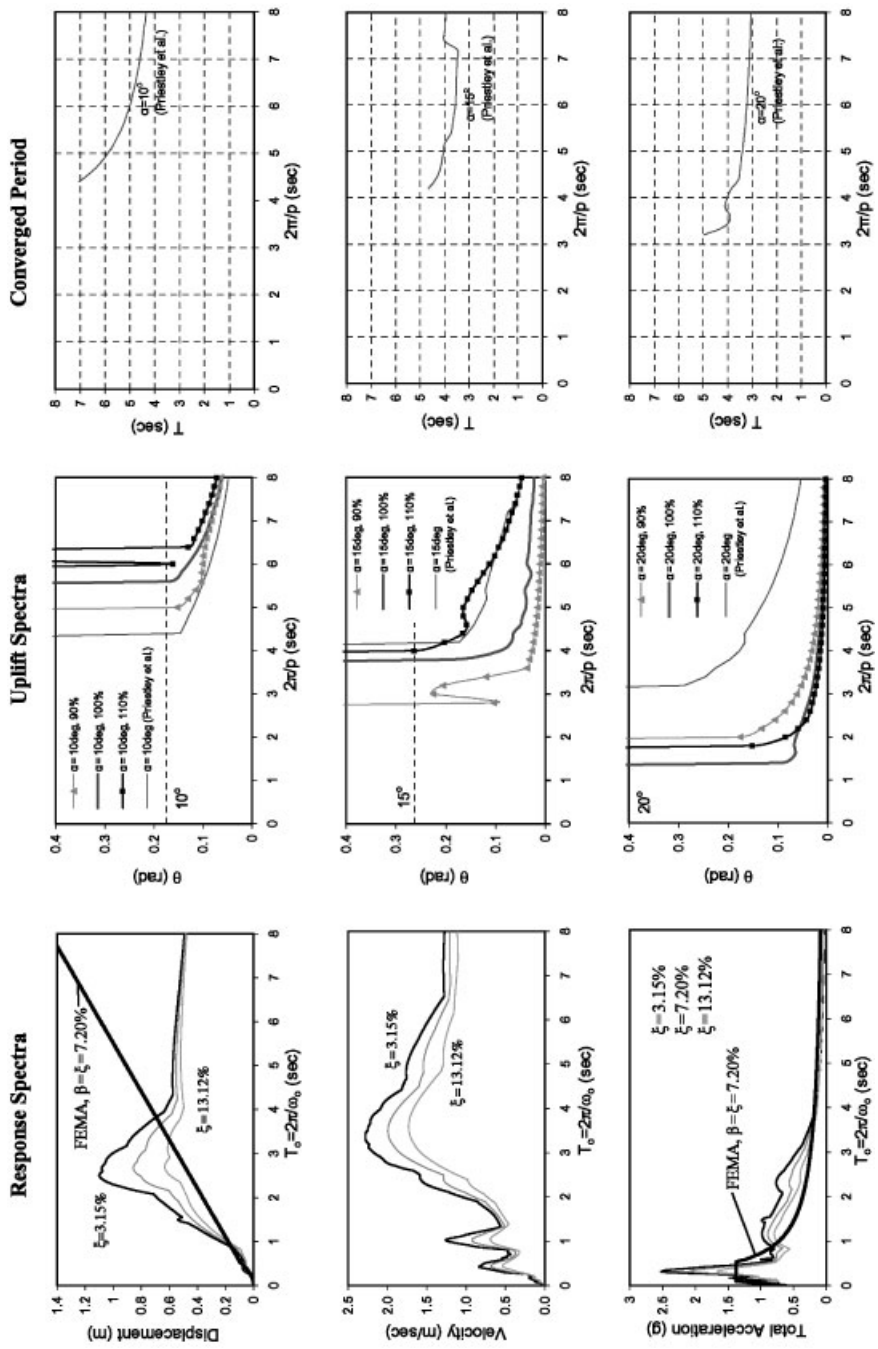

Figure 11. Comparison of exact and approximate uplift spectra (centre column) that have been computed with the Priestley *et al.* [8] method using the true displacement response spectrum (top left). The converged period that corresponds to the estimated uplift is shown in the right column. Ground Motion: Sylmar, 1994 Northridge.

THE FEMA 356 GUIDELINES

Under the chapter 'Foundation and Geologic Site Hazards', the Federal Emergency Management Agency (FEMA) 356 document *Prestandard and Commentary for the Seismic Rehabilitation of Buildings* [9] recommends as a possible procedure for estimating rotations of rocking structures the approximate procedure examined in the previous section of this report. The only difference in the FEMA recommendation is that instead of the exact displacement spectra used in Figures 6 and 8–11, one should use the FEMA design acceleration spectra, such as those shown in the bottom left of Figures 2, 3, 6, and 8–11, modified for the equivalent viscous damping of the rocking block in question.

$$\beta = 0.4(1 - \sqrt{r}) \tag{14}$$

where $\sqrt{r}$ is the coefficient of restitution given by Equation (4). The spectral displacement values needed to extract the rotations θ_i from Equation (13) are obtained from Equation (2). For the FEMA-recommended empirical expression (14) that furnishes the design value of the equivalent damping ratio, we do not have information on its origin. The resulting values of β from Equation (14) are plotted in Figure 5 with a dashed line together with the values of β prescribed by Equations (10) and (11). It is shown that the FEMA expression yields values of β which are about one-half the values of β predicted by Equation (10).

Figures 12 and 13 compare the predictions of the FEMA recommendations with the exact spectra. Note that for all five U.S. earthquake motions examined in this study, the FEMA recommendation predicts overturning of all blocks with slenderness $\alpha = 10^\circ$ and as large as $2\pi/p = 8$. For values of $\alpha = 15$ and 20°, the FEMA procedure grossly overestimates rotations to the extent that they are of no use. The FEMA procedure grossly overestimates the rotations even when the exact spectrum for 110% level of the record is used for comparison. For the Los Gatos record (right column of Figure 12), the FEMA guideline predicts overturning of all blocks as large as $2\pi/p = 8$ for $\alpha = 10,\ 15$, and 20°. Consequently, the concept of estimating rotations of rocking blocks by using response spectra and, in particular, design spectra should be abandoned.

CONCLUSIONS

This paper examines in depth the fundamental differences between the oscillatory response of a single-degree-of-freedom (SDOF) oscillator (regular pendulum) and the rocking response of a slender rigid block (inverted pendulum).

Initially the paper examines the underlying differences in the restoring mechanisms, stiffness, and damping values of the SDOF oscillator and the rocking block. Subsequently, the paper proceeds by examining the differences appearing in the free- and forced-vibration response of the two systems by emphasizing the nonlinear nature and sensitivity of the dynamic response of the rocking block. It is concluded that the SDOF oscillator and the rocking block are two fundamentally different dynamical systems, and the response of one should not be used to draw conclusion on the response of the other. This conclusion motivated the proposal to use the rocking spectra as an additional measure of earthquake intensity. Together with the response spectra, rocking spectra can provide a more lucid picture of the kinematic characteristics of ground motions and their implications on the response of rigid, yet slender, structures. The

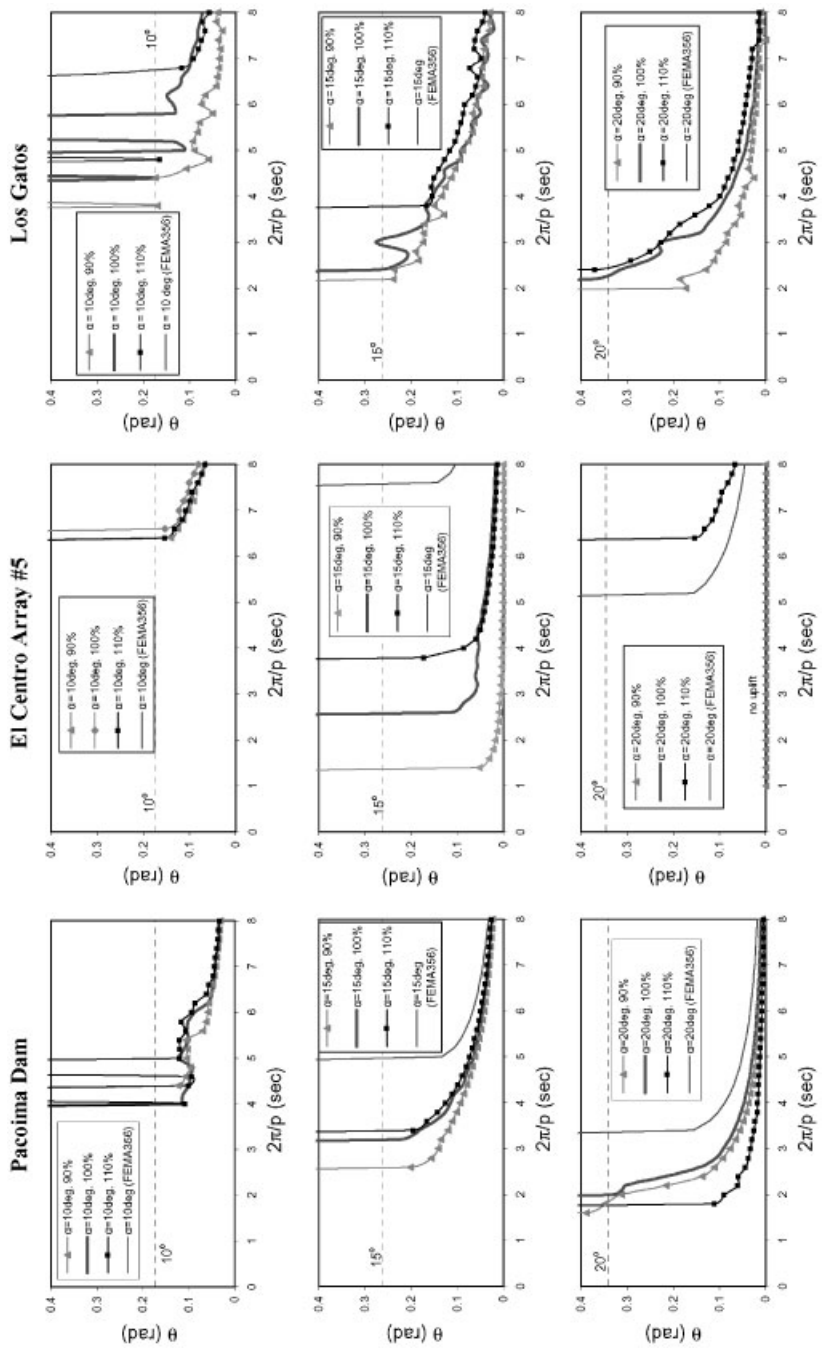

Figure 12. Comparison of exact and design uplift spectra that have been computed with the Priestley *et al.* [8] method using the FEMA design displacement spectra. When the thin solid line is not shown, the FEMA procedure predicts overturning over the entire $2\pi/p$ range shown.

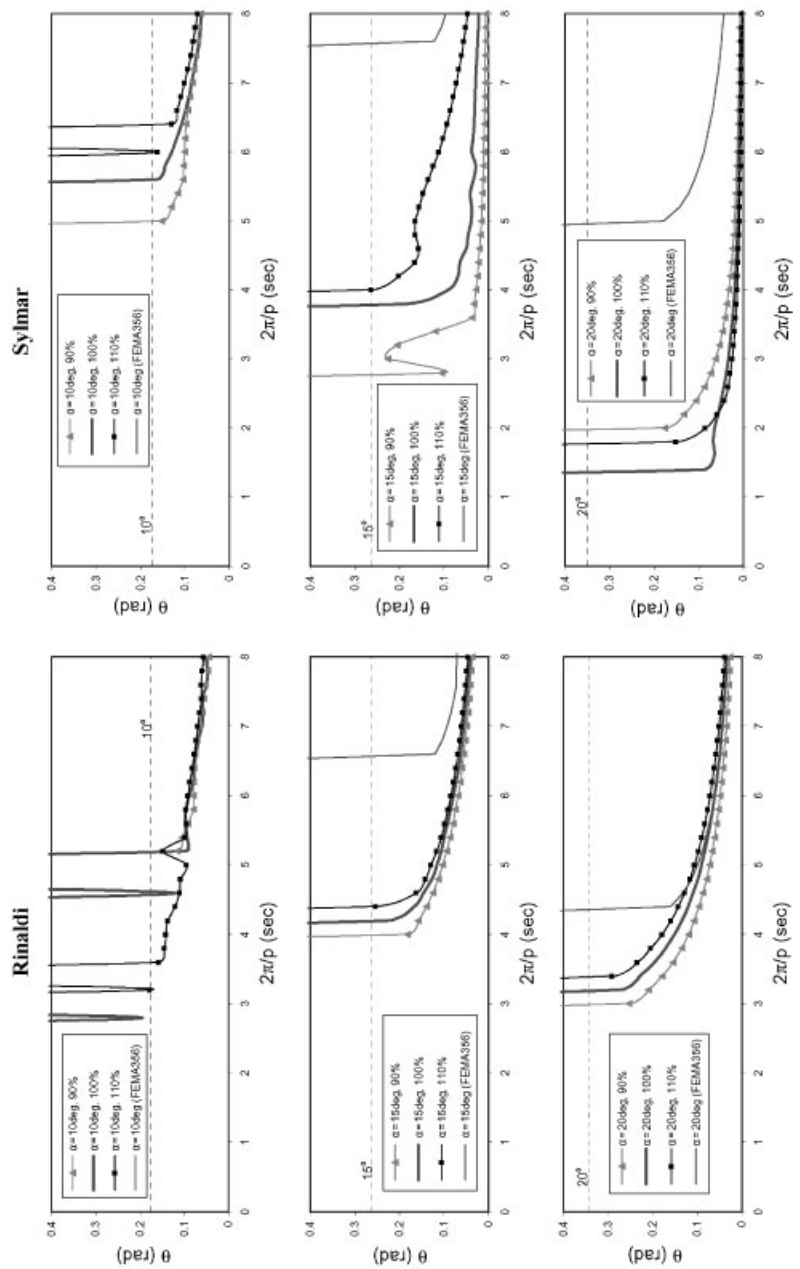

Figure 13. Comparison of exact and design uplift spectra that have been computed with the Priestley *et al.* [8] method using the FEMA design displacement spectra. When the thin solid line is not shown, the FEMA procedure predicts overturning over the entire $2\pi/p$ range shown.

exact response spectra were computed with 90, 100, and 110% of the acceleration level of the recorded motions. It was found that occasionally a lower level of excitation will produce higher rotations; however the rotation spectra exhibit noticeable order.

The paper examines in depth the validity of a two-decade-old approximate design methodology to estimate block rotations by performing iterations on the true or design displacement response spectrum of oscillating structures. It is shown that the approximate method is fundamentally flawed and should be abandoned.

ACKNOWLEDGEMENTS

Part of this work was conducted during a one-semester-long sabbatical leave of the senior author from the University of California at Berkeley. Partial financial support for this study was provided by the National Science Foundation under Grant CMS-0116354. The suggestion of both anonymous reviewers to include the rocking spectra for the 90 and 110% of the earthquake records is appreciated.

REFERENCES

1. Milne J. Seismic experiments. *Transactions of the Seismological Society of Japan* 1885; **8**:1–82.
2. Housner GW. The behaviour of inverted pendulum structures during earthquakes. *Bulletin of the Seismological Society of America* 1963; **53**(2):404–417.
3. Yim SCS, Chopra AK, Penzien J. Rocking response of rigid blocks to earthquakes. *Earthquake Engineering and Structural Dynamics* 1980; **8**(6):565–587.
4. Hogan SJ. On the dynamics of rigid block motion under harmonic forcing. *Proceedings of the Royal Society of London*, Series A 1989; **425**:441–476.
5. Shenton HW, III. Criteria for initiation of slide, rock, and slide-rock rigid-body modes. *Journal of Engineering Mechanics* (ASCE) 1996; **122**(7):690–693.
6. Makris N, Roussos Y. Rocking response of rigid blocks under near-source ground motions. *Géotechnique* 2000; **50**(3):243–262.
7. Zhang J, Makris N. Rocking response of free-standing blocks under cycloidal pulses. *Journal of Engineering Mechanics* (ASCE) 2001; **127**(5):473–483.
8. Priestley MJN, Evison RJ, Carr AJ. Seismic response of structures free to rock on their foundations. *Bulletin of the New Zealand National Society for Earthquake Engineering* 1978; **11**(3):141–150.
9. FEMA 356. *Prestandard and Commentary for the Seismic Rehabilitation of Buildings.* Prepared by the American Society of Civil Engineers for the Federal Emergency Management Agency. FEMA, Washington, DC, 2000.
10. Chopra AK. *Dynamics of Structures*: *Theory and Applications to Earthquake Engineering* (2nd edn). Prentice-Hall: Englewood Cliffs, NJ, 2000.
11. Clough R, Penzien J. *Dynamics of Structures* (2nd edn). McGraw-Hill: New York, NY, 1993.
12. *1997 Uniform Building Code.* Vol. 2 (Chapter 16). *International Conference of Building Officials*. Whittier, CA, 1997.
13. MATLAB Version 5.3. *The Language of Technical Computing.* The Mathworks, Inc.: Natick, MA, 1999.
14. Makris N, Zhang J. Rocking response and overturning of anchored equipment under seismic excitation. *Report No. PEER*-98/05, Pacific Earthquake Engineering Research Center, University of California, Berkeley, CA, 1999.
15. Makris N, Konstantinidis D. The rocking spectrum and the shortcomings of design guidelines. *Report No. PEER*-01/07, Pacific Earthquake Engineering Research Center, University of California, Berkeley, CA, 2001.

